Eur J Nucl Med Mol Imaging (2008) 35:589–597
DOI 10.1007/s00259-007-0586-z

ORIGINAL ARTICLE

Cerebral A_1 adenosine receptors (A_1AR) in liver cirrhosis

Christian Boy · Philipp T. Meyer · Gerald Kircheis · Marcus H. Holschbach · Hans Herzog · David Elmenhorst · Hans Juergen Kaiser · Heinz H. Coenen · Dieter Haussinger · Karl Zilles · Andreas Bauer

Received: 18 August 2006 / Accepted: 20 August 2007 / Published online: 14 November 2007

Abstract
Purpose The cerebral mechanisms underlying hepatic encephalopathy (HE) are poorly understood. Adenosine, a neuromodulator that pre- and postsynaptically modulates neuronal excitability and release of classical neurotransmitters via A_1 adenosine receptors (A_1AR), is likely to be involved. The present study investigates changes of cerebral A_1AR binding in cirrhotic patients by means of positron emission tomography (PET) and [^{18}F]CPFPX, a novel selective A_1AR antagonist.
Methods PET was performed in cirrhotic patients (n=10) and healthy volunteers (n=10). Quantification of in vivo receptor density was done by Logan's non-invasive graphical analysis (pons as reference region). The outcome parameter was the apparent binding potential (aBP, proportional to B_{max}/K_D).
Results Cortical and subcortical regions showed lower A_1AR binding in cirrhotic patients than in controls. The aBP changes reached statistical significance vs healthy controls ($p<0.05$, U test with Bonferroni-Holm adjustment for multiple comparisons) in cingulate cortex (−50.0%), precentral gyrus (−40.9%), postcentral gyrus (−38.6%), insular cortex (−38.6%), thalamus (−32.9%), parietal cortex (−31.7%), frontal cortex (−28.6), lateral temporal cortex (−28.2%), orbitofrontal cortex (−27.9%), occipital cortex (−24.6), putamen (−22.7%) and mesial temporal lobe (−22.4%).
Conclusion Regional cerebral adenosinergic neuromodulation is heterogeneously altered in cirrhotic patients. The decrease of cerebral A_1AR binding may further aggravate neurotransmitter imbalance at the synaptic cleft in cirrhosis and hepatic encephalopathy. Different pathomechanisms may account for these alterations including decrease of A_1AR density or affinity, as well as blockade of the A_1AR by endogenous adenosine or exogenous xanthines.

Keywords Cirrhosis · Brain receptors and neurotransmitters · Positron emission tomography · Adenosine · [^{18}F]CPFPX

Christian Boy and Philipp T. Meyer contributed equally to this work.

C. Boy · P. T. Meyer · H. Herzog · D. Elmenhorst · K. Zilles · A. Bauer (✉)
Brain Imaging Centre West, Institute of Medicine, Research Centre Jülich, Jülich, Germany
e-mail: an.bauer@fz-juelich.de

A. Bauer
Department of Neurology, University of Düsseldorf, Düsseldorf, Germany

G. Kircheis · D. Haussinger
Clinic for Gastroenterology, Hepatology and Infectiology, University of Düsseldorf, Düsseldorf, Germany

M. H. Holschbach · H. H. Coenen
Institute of Nuclear Chemistry, Research Centre Jülich, Jülich, Germany

K. Zilles
C. & O. Vogt Institute of Brain Research, Düsseldorf, Germany

H. J. Kaiser
Department of Nuclear Medicine, University Hospital Aachen, Aachen, Germany

Present address:
P. T. Meyer
Department of Nuclear Medicine, University Hospital Aachen, Aachen, Germany

Present address:
C. Boy
Department of Nuclear Medicine, University Hospital Essen, Essen, Germany

Introduction

Hepatic encephalopathy (HE) is a neuropsychiatric syndrome occurring in acute or chronic liver disease. A common cause of HE is alcoholic or viral liver cirrhosis associated with portal hypertension and/or portal-systemic shunts [1–7]. An altered sleep–wake cycle, fatigue, cognitive and motor deficits are among the symptoms of HE [3, 5–11]. HE is functional in nature, potentially reversible and precipitated by heterogeneous factors, e. g., ammonia, benzodiazepines, inflammatory cytokines and hyponatremia [3, 6, 12, 13]. Current evidence suggests that HE is the consequence of a low-grade chronic glial oedema with subsequent alterations of glio-neuronal interaction and cerebral neurotransmission [1, 3, 6, 7, 14].

It was hypothesized that astrocyte swelling integrates some actions of HE-relevant toxins leading to impaired astrocyte function in HE [1, 2]. Recent findings suggest a close relationship between astrocyte swelling, glutamate, NMDA receptor signalling, oxidative stress, and nitric oxide, which may result in mutual amplification of swelling and oxidative stress [3]. In experimental HE, changes of gene expression were shown for different neurotransmitter systems, e.g. glutamate, gamma amino butyric acid (GABA), serotonin, dopamine, histamine, opioids, adrenaline and acetylcholine, suggesting that an imbalance of excitatory and inhibitory neurotransmission is a relevant molecular mechanism of HE [14].

Experimental observations [14] and clinical findings [15, 16] have led to our hypothesis that regional cerebral purinergic neuromodulation is altered in cirrhosis: first, adenosine is a key player in sleep regulation [17]. A high prevalence of sleep disturbances in cirrhosis [18], which is likely to impair alertness and general arousal of the cerebral cortex [10, 19], has implied a pathogenetic involvement of adenosine. Moreover, adenosine has a central role in the modulation of cerebral neurotransmission, as it inhibits the release of different neurotransmitters relevant for HE, e.g. glutamate, GABA, serotonin, via presynaptic A_1AR [14, 15, 20, 21]. Moreover, A_1AR activation is postulated to be protective against glutamate excitotoxicity [20]. Finally, hepatic metabolism of xanthines (acting via A_1AR) may be altered in cirrhosis [16]. Based on the assumption that in cirrhosis an imbalance of neurotransmitters and oxidative stress [6, 7, 22] interferes with cerebral adenosinergic neuromodulation, the present study investigated changes of A_1AR binding in cirrhotic patients using positron emission tomography (PET) and the novel subtype-selective A_1AR-antagonist [^{18}F]CPFPX [23].

Materials and methods

Human subjects

The study protocol conformed to the ethical guidelines of the 1975 Declaration of Helsinki as reflected in a priori approval by the Ethics Committee of the Medical Faculty of the University of Düsseldorf, Germany. Written informed consent was obtained from all subjects. Ten patients with liver cirrhosis (five women, five men; age range 35.3–69.6 years, mean 49.3±9.3 years) participated in the PET study. Cirrhosis was diagnosed histologically in all cases. Demographic and clinical data, results of computerized psychometric tests and HE classification are summarized in Tables 1 and 2.

The severity of HE in patients was graded according to the established West-Haven criteria and by using the psychometric test battery. Resulting test parameters were considered abnormal when they were outside 1 standard deviation (SD) from the mean of a large age-matched control population. A psychometric test was considered abnormal when one or more of its test parameters was abnormal. The tests that were used in the present study have been described previously in detail [9, 10, 24]. Patients without evidence of manifest HE according to the mental state (West-Haven criteria) were defined to have HE 0 when none or only one of the computerized psychometric tests was abnormal; patients were classified as minimal HE (mHE) when two or more of the five computerized psychometric tests were abnormal (Table 2) [9, 10].

Patients with manifest HE were classified as HE I or HE II according to mental state gradation. Visual discrimination ability and general arousal of the neocortex were assessed by determination of critical flicker frequency (CFF) thresholds and used here for further quantification of HE severity in cirrhotic patients with little age, day-time and training dependency [7, 9, 10]. Grading of HE was performed by the same investigator, who was blinded to the CFF results. Exclusion criteria were the presence of severe HE (grades higher than HE II), obvious alcohol abuse during the last 6 months, overt neurological or psychiatric diseases except HE, drug abuse, intake of psychoactive drugs, acute gastrointestinal haemorrhage or spontaneous bacterial peritonitis during the past 7 days and significant extra-hepatic disease, such as heart failure or renal insufficiency.

Ten age-matched healthy human volunteers (five women, five men; age range 36.5–68.4 years, mean 48.9±10.4 years) were included as control population. Volunteers were screened for history of medical illness, especially internal, neurological and psychiatric diseases, head injury,

Table 1 Demographic, laboratory and computerpsychometric data of cirrhotic patients (P1–P10)

Cirrhotic patient	Age (years), sex	Etiology of cirrhosis	Child-Pugh (pts)	Albumin (g/l)	Bilirubin total (μmol/l)	GGT (U/l)	Prothrombin time (%)	Na (mmol/l)	Ascites	Survival, maximum HE grade during follow up
P1	35.3, M	Alcohol	B9	32	234.3	415	55	130	Yes	†*HE IV
P2	46.8, M	Alcohol	A5	41	10.3	142	95	142	Absent	Alive, mHE
P3	47.6, M	Alcohol	A6	35	36.8	58	90	137	Absent	Alive, mHE
P4	50.9, F	HCV	A5	39	26.8	8	83	143	Absent	Alive, mHE
P5	50.5, M	Alcohol	C11	24	314.9	39	39	134	Yes	Alive, mHE
P6	44.6, F	Alcohol	B9	41	22.2	57	68	134	Yes	†*HE IV
P7	42.1, F	Alcohol	B9	33	46.9	29	79	137	Yes	Alive, HE I
P8	47.4, F	HCV	A6	37	5.8	30	103	138	Absent	Alive, HE I
P9	57.8, F	Alcohol	B10	27	21.2	92	79	137	Yes	†HE IV
P10	69.6, M	Alcohol	C10	28	26.5	204	81	129	Yes	†HE IV

M male, *F* female, *HCV* hepatitis C virus, *GGT* gamma-glutamyl transferase, *n.d.* not determined
†Deceased
*Postmortem brain examination of A_1AR density
‡abnormal test parameter

alcohol or substance abuse (including nicotine and cannabis) and current medication use. Beginning with the entire day preceding the PET until the end of the imaging, caffeine intake was prohibited for all healthy and cirrhotic subjects.

Radiosynthesis, PET and MRI scanning

Radiosynthesis and formulation of [^{18}F]CPFPX were performed as previously described [23]. The tracer was dissolved in a volume of 10 ml sterile saline. At the time of injection, mean specific radioactivity was 71.8±57.9 GBq/μmol (range 14.8–265.6 GBq/μmol). Mean injected radioactivity was 256.9±7.4 MBq (range 243.1–266.4 MBq) in patients and 252.7±6.7 MBq (range 239.1–260.9 MBq) in controls, respectively. In all cases, the mass of injected CPFPX was below 16.6 nmol (equal to 5.3 μg). PET measurements were performed in 3D mode on a Siemens ECAT EXACT HR+ scanner (Siemens-CTI, Knoxville, TN, USA).

Scatter from outside the field of view was reduced by insertion of a lead shield into the scanner gantry. A 10-min

Table 2 HE classification, laboratory test results and computerpsychometric data of cirrhotic patients (P1–P10)

Cirrhotic patient	HE grade	CFF (Hz)	Arterial ammonia (mmol/l)	NCT-A time (s)	Aiming time (s)	Visual pursuit test		Cognitrone		TAVTMB	
						Time/correct hit [s]	Correct hits [*n*]	Time/correct hit [s]	Correct hits [*n*]	Correct symbols [*n*]	Wrong symbols [*n*]
P1	HE0	39.1	56	23	11.8‡	3.9	40	2.2	78	52	1
P2	HE0	40.8	74	35	8.5	3.7	40	3.1	76	38‡	9‡
P3	mHE	42.0	69	33	10.1	4.1	38‡	2.5	72‡	45	3
P4	mHE	39.0	39	28	9.0	3.5	31‡	2.1	72‡	51	8‡
P5	mHE	41.5	n.d.	n.d.	14.1‡	5.1	39	3.0	67‡	42	4
P6	HE I	38.7	49	30	9.5	5.5‡	35‡	4.8‡	78	49	10‡
P7	HE I	38.8	35	32	9.5	4.5	37‡	3.6	75	36‡	2
P8	HE I	34.9	27	48	13.4‡	5.7‡	39	3.5	66‡	50	13‡
P9	HE I	36.4	99	40	12.0‡	4.7	37‡	2.9	74	43	6
P10	HE II	27.4	81	n.d.	n.d.	n.d.	n.d.	n.d.	n.d.	n.d.	n.d.

Test results of five psychometric tests (1–5) are displayed: (1) NCT-A, Number Connection Test-A, (2) Aiming, i.e. a motor performance series for evaluation of fine-motoric abilities, (3) Visual Pursuit Test, test for registration of concentrated, targeted visual perception, (4) Cognitrone, test for evaluation of attention and concentration, and (5) TAVTMB, tachystoscopic traffic-perception test Mannheim for Screen.
M male, *F* female, *HCV* hepatitis C virus, *GGT* gamma-glutamyl transferase, *CFF* critical flicker frequency, *n.d.* not determined, ‡ abnormal test parameter

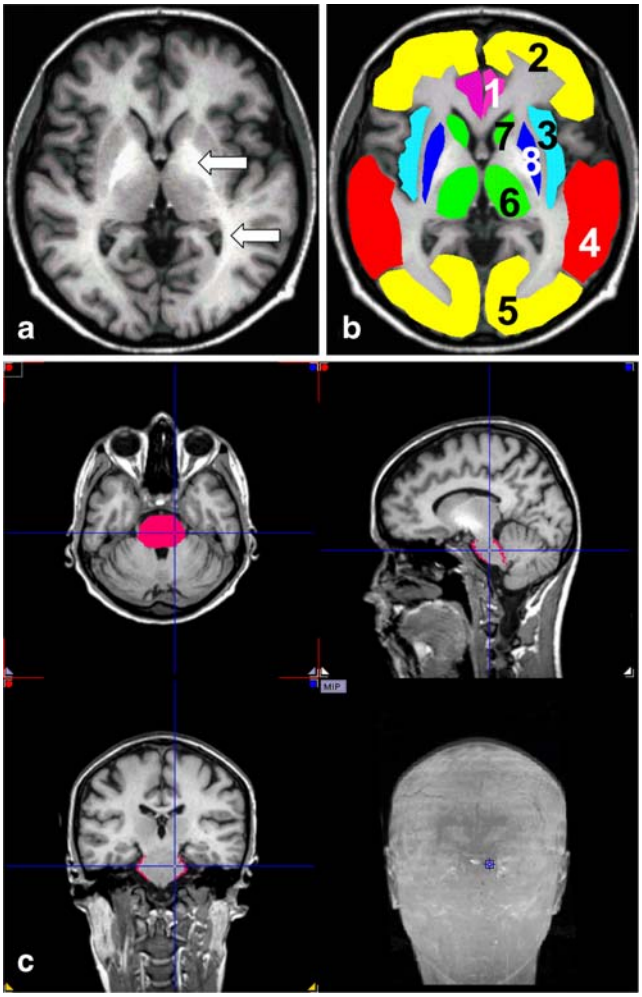

Fig. 1 **a**–**c** Anatomical MRI and definition of individual volumes of interest (PMOD-display). **a** T1-weighted magnetization-prepared rapid-acquisition gradient-echo sequence of a representative cirrhotic patient (P7) at the level of the basal ganglia (transversal plane). Note the bilateral white matter signal hyperintensities (*arrows*) as typically found in cirrhosis. **b** Volumes of interest were defined on the individual MRI: *1* cingulum, *2* frontal cortex, *3* insula, *4* temporal lateral cortex, *5* occipital cortex, *6* thalamus, *7* caudate nucleus, *8* putamen. **c** Here the pontine volume of interest and its anatomical borders are displayed in the respective planes: transversal (*top left*), sagittal (*top right*), and coronal (*bottom left*). MIP: maximum intensity projection (*bottom right*). The pons (*outlines* in *red colour*), served as reference region. The pons lies ventral to the cerebellum, below the midbrain and above the medulla with which it is superficially demarcated by a ventrolateral sulcus. The other anatomical borders are the cerebral and cerebellar pedunculi, the fourth ventricle, the interpeduncular and the pontine cisterns

transmission scan (^{68}Ge/^{68}Ga) was obtained for attenuation correction. PET acquisition (60 min) began with the start of [^{18}F]CPFPX injection as a bolus over 20 s. Dynamic emission data was acquired in 24 frames (frame length ranging from 10 to 600 s). PET data were corrected for randoms, scatters and attenuation, rebinned into 2D sinograms, and reconstructed by filtered back-projection (Shepp filter, cut-off=2.5 mm) with a voxel size of 2.0×2.0×2.4 mm^3 (63 slices).

MRI scans were obtained within the week of PET scanning on a Siemens Magnetom VISION 1.5-T scanner using a 3D T1-weighted magnetization-prepared rapid-acquisition gradient-echo sequence. Individual MRI data sets were aligned into anterior commissure–posterior commissure orientation using a 3D image registration software (MPITool, ATV Co., Germany). Subsequently, a summed PET image (5–60 min) was matched to the re-aligned MRI, and co-registration parameters were applied to each PET frame. Volumes of interest (VOI) were defined on individual transversal MRI planes for frontal cortex, orbitofrontal cortex, precentral gyrus, postcentral gyrus, parietal cortex, occipital cortex, lateral temporal cortex, mesial temporal lobe, insular cortex, cingulate cortex, caudate nucleus, putamen, thalamus and pons (Fig. 1) as described previously, and superimposed onto all PET frames with a dedicated software (PMOD, V2.4, PMOD Group, Switzerland) [25, 26].

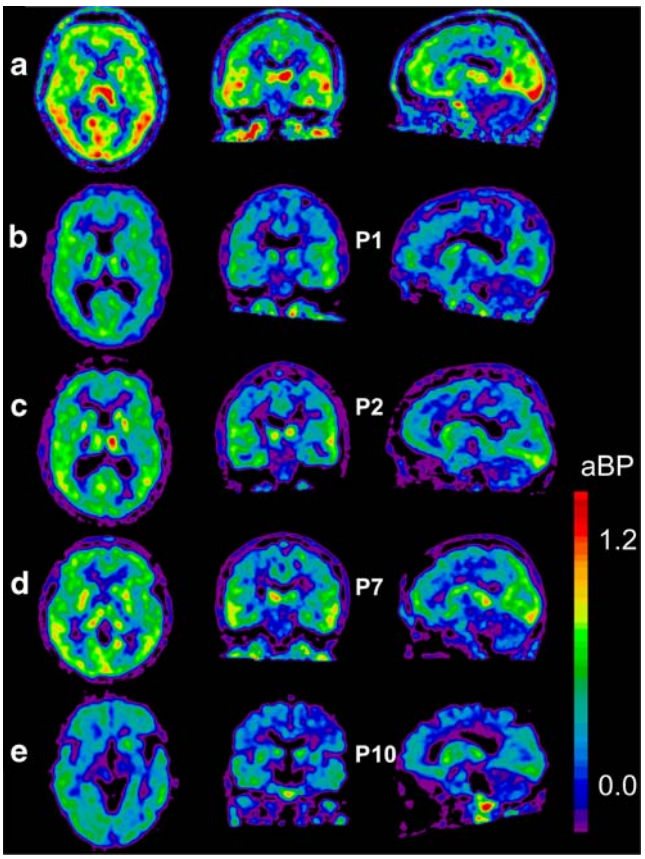

Fig. 2 **a**–**e** Parametric images of [^{18}F]CPFPX binding showing the cerebral distribution of A_1AR. **a** Normal distribution of A_1AR in a representative healthy volunteer (female, 40 years old). **b**–**e** Heterogeneous reductions of cortical and subcortical binding were evident in cirrhotic patients without or with a manifest HE. The individual HE grading of the patients displayed was: **b** HE 0 (P1), **c** minimal HE (P2), **d** HE I (P7), and **e** HE II (P10). Orthogonal planes (*from left*: transversal, coronal, and sagittal). *Bar*: apparent binding potential (aBP), linear scale

For each VOI regional side-averaged decay-corrected time-activity, curves were generated. The pons served as reference region (Fig. 1c), as pontine uptake mostly reflects free and non-specifically bound [^{18}F]CPFPX due to its low A_1AR concentration [27]. For kinetic analyses, Logan's non-invasive graphical analysis (GA) was applied [28]. The distribution volume ratio (DVR) is given by the slope of the linear part of the GA plot with a fixed starting point (from 20 min p. i.) [28]. The apparent binding potential (aBP), which is proportional to the ratio of receptor density to ligand affinity (B_{max}/K_D) was used as an outcome parameter reflecting A_1AR density (aBP=DVR−1) [26]. Parametric images were generated.

Statistical analysis

Data are expressed as mean ± SD. All statistical analyses were performed using SPSS (release 12.0.1, SPSS, Chicago, IL). Following one-way ANCOVA with age and sex as covariates, differences between the means of two variables were evaluated by the two-sided Mann–Whitney *U* test. HE grade and CFF were tested for correlation with aBP by two-sided Spearman rank correlation analysis; $P<0.05$ was considered statistically significant. To account for multiple comparisons, the Bonferroni-Holm method was applied.

Results

Figure 2a displays the parametric aBP image of a typical control subject. Binding of [^{18}F]CPFPX to A_1AR was heterogeneously reduced in cortex and subcortical brain regions of cirrhotic individuals, either without (Fig. 2b,c) or with a manifest HE (Fig. 2d,e). There were no influences of age or gender on the binding parameter aBP (ANCOVA, $p>0.05$). Table 3 summarizes mean aBP (± SD) values of cirrhotic patients and healthy volunteers for different brain regions. Significant reductions of aBP were present in cingulate cortex (−50.0%), precentral gyrus (−40.9%), postcentral gyrus (−38.6%), insular cortex (−38.6%), thalamus (−32.9%), parietal cortex (−31.7%), frontal cortex (−28.6), lateral temporal cortex (−28.2%), orbitofrontal cortex (−27.9%), occipital cortex (−24.6), putamen (−22.7%) and mesial temporal lobe (−22.4%).

By contrast, aBP did not differ significantly between cirrhotic patients and controls in caudate nucleus. In all regions, aBP neither correlated with HE grade ($P>0.05$) nor with CFF ($P>0.05$). Regional aBP tended to be negatively correlated with the Child-Pugh score (Fig. 3, Table 3) in ten of the 13 cortical (frontal, postcentral, parietal, occipital, lateral temporal, insular, cingulate and mesial temporal lobe) and subcortical regions (thalamus and caudate). However, when the Bonferroni-Holm method was applied, none of these correlations reached statistical significance. All cir-

Table 3 Apparent binding potential (aBP, mean ± SD) of the examined brain regions in cirrhotic patients vs controls

ABP	Controls ($n=10$)	Cirrhosis ($n=10$)	Cirrhosis vs Controls†	Correlation of aBP with Child Pugh score in cirrhosis‡	
Brain region			P(2-sided)	*R*	P (two-sided)
Frontal cortex	0.56±0.13	0.40±0.09	0.009*	−0.787	0.007
Orbitofrontal cortex	0.61±0.09	0.44±0.09	0.002*	−0.551	0.099
Precentral gyrus	0.44±0.12	0.26±0.09	0.002*	−0.526	0.118
Postcentral gyrus	0.44±0.13	0.27±0.07	0.007*	−0.774	0.009
Parietal cortex	0.60±0.14	0.41±0.10	0.002*	−0.681	0.030
Occipital cortex	0.65±0.09	0.49±0.10	0.002*	−0.718	0.019
Lateral temporal cortex	0.71±0.10	0.51±0.10	0.001*	−0.737	0.015
Mesial temporal lobe	0.49±0.07	0.38±0.09	0.007*	−0.712	0.021
Insular cortex	0.57±0.08	0.35±0.10	0.001*	−0.818	0.004
Cingulate cortex	0.56±0.13	0.28±0.08	0.001*	−0.768	0.009
Caudate nucleus	0.58±0.08	0.50±0.12	0.105	−0.774	0.009
Putamen	0.88±0.09	0.68±0.15	0.009*	−0.632	0.050
Thalamus	0.70±0.09	0.47±0.09	0.001*	−0.638	0.047

Rank correlation of aBP and Child-Pugh score in cirrhotic subjects: aBP of the 13 brain regions neither correlated with HE-grading nor with critical flicker frequency ($P>0.05$), while aBP tended to be inversely related to the Child-Pugh score.
†Mann–Whitney *U* test;
*Statistically significant after Bonferroni-Holm adjustment;
‡ A Spearman-rho correlation coefficient $|r|>0.5$ was considered relevant. After correction for multiple comparisons none of the observed correlations of aBP and Child-Pugh score remained statistically significant.

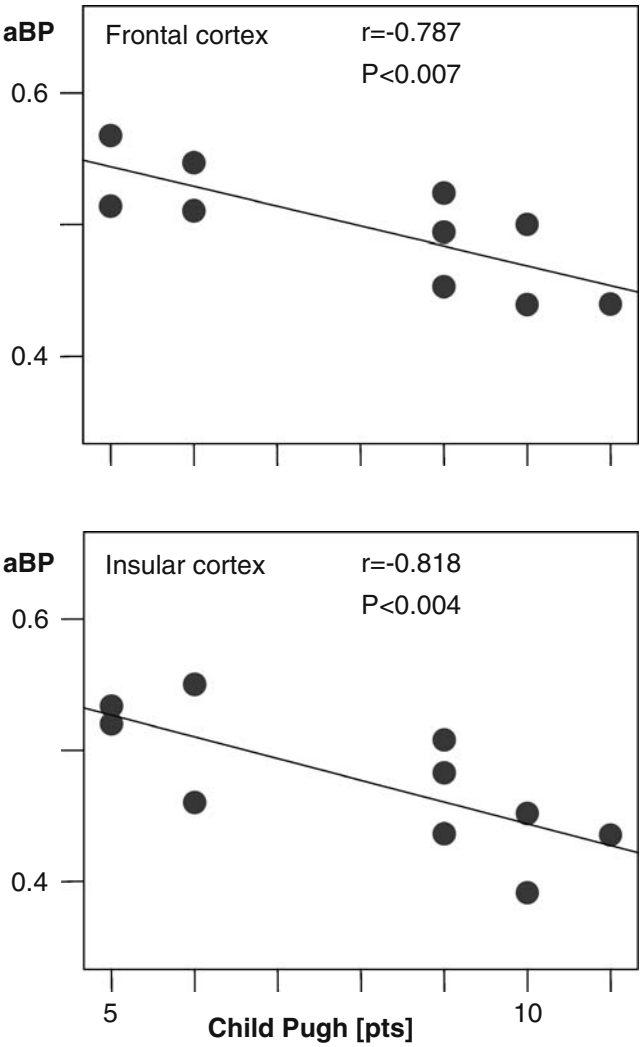

Fig. 3 Relation of the apparent binding potential (aBP) and Child-Pugh score in frontal and insular cortex of ten cirrhotic subjects. HE grade and CFF were tested for correlation with aBP by two-sided Spearman rank correlation analysis

rhotic patients showed symmetrical signal hyperintensities in T1-weighed MRI scans, especially in the globus pallidus and—to a varying degree—in other white-matter localisations (Fig. 1a,c).

Discussion

This is the first study on cerebral adenosine receptor changes in chronic liver disease in vivo. [^{18}F]CPFPX is a novel well-characterized and specific PET ligand to map cerebral A_1AR [23, 26, 29–35]. In contrast to other adenosine receptor subtypes (A_{2A}, A_{2B}, and A_3), the A_1AR is expressed throughout the brain with high density (except pons and cerebellum with A_1AR concentrations at very low levels) [20, 27, 29]. It is a fact that there is no ideal reference region in the human brain that is completely devoid of A_1ARs [32, 34]. It is therefore not possible to determine the concentration of free and non-specifically bound ligand directly.

We have previously described measurement of A_1AR binding using [^{18}F]CPFPX and an invasive protocol with arterial blood sampling [28]. It has been shown for other ligands that a small amount of specific binding in the reference region does not exclude the application of a reference tissue model [34]. In a recent work using [^{18}F]CPFPX in humans, various outcome parameters were compared based on either metabolite-corrected venous blood sampling (e.g. apparent equilibrium total distribution volume [DVt′]) or a reference region (ratio of specific to non-specific distribution volume [BP2]) [34]. As a result, quantification of [^{18}F]CPFPX imaging has appeared to be reproducible and reliable for PET studies of the cerebral A_1AR [34]. Moreover, among the outcome parameters, the non-invasive measures were of superior test–retest stability compared with the invasive measures [34].

In normal volunteers as presented here, cerebral accumulation and binding of [^{18}F]CPFPX corresponded well to the known distribution pattern of A_1AR in healthy individuals as obtained from previous in vitro studies using other ligands [27] as well as in vivo and in vitro studies using this ligand in humans [26, 29–35]. The non-invasive graphical analysis for quantification of aBP does not require arterial blood sampling to determine the plasma input function, which would be unsuitable in cirrhotic patients with compromised blood coagulation. Moreover, a bolus-infusion protocol to assess receptor binding under equilibrium conditions or a graphical analysis using venous blood data is not applicable because of the altered hepatic metabolism of [^{18}F]CPFPX in cirrhosis [29–35]. Pons was selected as reference region, as in cirrhotic patients pontine glucose metabolism and perfusion have not displayed alterations under baseline conditions or while performing cognitive tasks [5, 6, 8, 9]. It is known that the pons is less sensitive to alcohol-related brain damage than the cerebellum, which is another putative reference region [36].

Moreover, the observed region-dependent and heterogeneous distribution pattern of aBP changes in cirrhosis with reductions in the range of 22 to 50% cannot be simply explained by a systematic error due to an altered binding of [^{18}F]CPFPX in the reference region, which would rather cause a more homogeneous shift of aBP. To avoid an age-related bias of the group comparisons, we used age-matched control subjects. Despite the frequent observation of an age-dependent decrease of G-protein-coupled neuroreceptors, as shown for A_1ARs in rodents (by means of quantitative autoradiography) [26] and in humans (with PET and [^{18}F]CPFPX) [37], our data did not detect any influence of age or gender on the aBP. This may be due to the relatively small

sample size and the narrow age range. Morhophologically, all cirrhotic patients showed typical T1-signal hyperintensities, especially within the pallidum, which have been attributed to manganese deposition [38].

Our results indicate that cerebral A_1AR binding is reduced in cortical and subcortical regions of cirrhotic individuals with different severities of hepatic encephalopathy. Reductions of aBP are present to a different extent in functionally relevant areas related to motor and cognitive impairments caused by HE [6–9, 11, 36, 38]. It may be hypothesized that in cirrhosis a loss or dysfunction of cerebral A_1AR reflects or further aggravates neurotransmitter imbalance, in particular, that of glutamate and monoaminergic transmitters [5, 6, 14, 20]. Recent experimental and clinical data of patients who died from cirrhosis have provided evidence for an augmented glutamate-nitric oxide-cyclic guanosine monophosphate (cGMP) pathway involving frontal cortex and cerebellum [22]. Furthermore, experimental HE models have suggested beneficial effects of glutamatergic *N*-methyl-*d*-aspartate (NMDA) receptor antagonists or pharmacological manipulation of the glutamate-nitric oxide-cGMP pathway [39, 40].

The detected aBP reductions may be caused by an A_1AR loss due to atrophy, a diminished A_1AR expression, and by alterations of the receptor-to-ligand coupling with any combination of these factors: first, a loss of A_1AR expressing neurons is less likely as simple explanation of our results, as HE is not a primary consequence of extensive neuronal cell death, especially in early stages [6]. Furthermore, in our ten patients vs age-matched controls, we found a regional pattern of aBP reductions that did not mimic the known pattern of alcohol-related grey-and-white matter atrophy [36, 39]. Finally, increased extracellular adenosine levels may also account for the observed changes and competitive A_1AR blockade: it has been shown that exposure to the endogenous agonist adenosine leads to long-term desensitization of recombinant human A_1ARs by both decreased coupling of receptors to G-proteins and by down-regulation of receptor number [40].

Likewise, a blockade of A_1AR by exogenous xanthines—especially caffeine—may also reduce aBP of [^{18}F]CPFPX, as plasma caffeine clearance is prolonged in cirrhosis [15, 35, 40]. Recently, Matusch et al. have reported a reduced clearance of the PET ligand used in this study: the metabolism of [^{18}F]CPFPX was impaired in a patient with liver cirrhosis accompanied by higher blood levels of the non-metabolized ligand and altered regional time–activity curves, respectively [35].

Our present in vivo data on A_1AR in cirrhosis is in good agreement with very recent postmortem receptor autoradiography performed in two patients of the present study who died in hepatic coma (i.e. patient P1 and patient P6), which also revealed significant decreases of the A_1AR density (B_{max}), in cortex and subcortex (Tables 4 and 5) by 25 to 60% [41]. Using consecutive postmortem brain slices of four cirrhotic subjects suffering from HE and aged 55± 16 years. Palomero-Gallagher et al. [41] quantified B_{max} of different receptors for classical neurotransmitters and adenosine: glutamate (ionotropic AMPA, kainate, NMDA, metabotopic mGLU 2/3), GABA ($GABA_A$, $GABA_B$, benzodiazepine-binding site), acetylcholine (muscarinic M1, M2, M3 and nicotinic), noradrenaline (α_1, α_{2h}), serotonin (5-$HT1_A$, 5-HT2), dopamine (D_1, D_2), and adenosine (A_1,A_{2A}). A main finding was that in the state of cirrhosis and HE (n=4) significant changes of B_{max} exclusively afflicted A_1AR (decrease) and NMDA, (increase) in precentral cortex [41]. In the putamen several receptor subtypes showed significant involvement as reflected by decreases of A_1AR, A_{2A}, kainate, NMDA, $GABA_B$, 5-$HT1_A$, and D_1 [41].

Table 4 A_1AR in cirrhosis: individual aBP measured by PET in two cirrhotic patients (P1 and P6)

ABP	Patient P1	Patient P6	Control, age matched, n=10
Brain region			
Precentral cortex	0.25	0.18	0.44±0.12
Putamen	0.53	0.52	0.88±0.09

Cortical (precentral, i.e. primary motor) and subcortical (putamen) PET results are compared to control.

However, although Palomero et al. used quantitative receptor autoradiography according to methodological standards [41] this approach was not due to determine KD for patients and controls given in Tables 4 and 5. Consequently, not only changes in the expression of A_1AR, but also changes of ligand affinity A_1AR may have occurred in cirrhosis. It has to be acknowledged that KD could change with a progression of disease and as such could introduce a confounding variable to results.

Despite our initial expectation, we did not observe any significant correlation of regional aBP and HE grade or CFF, respectively. On the other hand, aBP tended to be inversely related to the patient's Child-Pugh score, which increases with higher HE grades. At present, it seems likely that the changes in A_1AR binding precede the development

Table 5 A_1AR in cirrhosis: post mortem B_{max} of two patients (P1 and P6) measured for precentral cortex and putamen*

B_{max} [fmol/mg protein]	Patient P1	Patient P6	Control, age-matched, n=3
Brain region			
Precentral cortex	591	547	794±47
Putamen	451	412	817±33

*Post mortem B_{max} data reported by Palomero-Gallagher et al. [41].

of a manifest or minimal HE in cirrhosis. The presented observations in cirrhotic patients have provided further evidence for an altered neurochemical environment in the metabolically impaired brain [6]. It is concluded that, in addition to the known changes within the astrocytes, a reduced binding of [^{18}F]CPFPX reflects a presumably early impairment of adenosinergic neuromodulation in chronic liver disease [1–3, 6, 7].

It may be hypothesized that the involvement of A_1AR is functionally relevant in the context of a multifactorial and multisite pathogenesis of HE afflicting glia, neurons, microvasculature and extracellular space [1–3, 5–7]. At the molecular level, the interaction of a reduced cerebral A_1AR binding an altered brain function and the development of HE remains to be elucidated and should be subject for further investigations. In this respect, longitudinal studies with higher numbers of cirrhotic patients with different HE grades as well as experimental data would be needed. Strategies targeting adenosine, A_1AR and xanthines and glutamate to reduce neurotransmitter imbalance may potentially be beneficial in the treatment of cirrhotic patients in addition to conventional therapeutic concepts of HE [5, 12, 13, 15, 40, 42–44].

Acknowledgements This study was supported by grants from the German Research Foundation (DFG) through the Collaborative Research Centre 575 (Experimental Hepatology, C5), and the Federal Ministry of Education and Research (Neuroimaging, Brain Imaging Centre West). The authors thank E. Theelen, S. Schaden, L. Tellmann, B. Elghahwagi, K. H. Beyer, and G. Oeffler (Institute of Medicine), M. Lang, B. Palm, and E. Wabbals (Institute of Nuclear Chemistry) for excellent technical assistance and Dr. W. Meyer (Central Institute for Applied Mathematics, Research Centre Jülich) for statistical consultation.

References

1. Haussinger D, Laubenberger J, vom Dahl S, Ernst T, Bayer S, Langer M, et al. Proton magnetic resonance spectroscopy studies on human brain myo-inositol in hypo-osmolarity and hepatic encephalopathy. Gastroenterology 1994;107:1475–80.
2. Haussinger D, Kircheis G, Fischer R, Schliess F, vom Dahl S. Hepatic encephalopathy in chronic liver disease: a clinical manifestation of astrocyte swelling and low-grade cerebral oedema? J Hepatol 2000;32:1035–8.
3. Haussinger D, Schliess F. Astrocyte swelling and protein tyrosine nitration in hepatic encephalopathy. Neurochem Int 2005;47:64–70.
4. Ferenci P, Lockwood A, Mullen K, Tarter R, Weissenborn K, Blei AT. Hepatic encephalopathy-definition, nomenclature, diagnosis, and quantification: final report of the working party at the 11th World Congresses of Gastroenterology, Vienna, 1998. Hepatology 2002;35:716–21.
5. Butterworth RF. Pathogenesis of hepatic encephalopathy: new insights from neuroimaging and molecular studies. J Hepatol 2003;39:278–85.
6. Butterworth R. Metabolic encephalopathies. In: Siegel GJ, Albers RW, Brady ST, Price DL, editors. Basic neurochemistry: molecular, cellular, and medical aspects. 7th ed. San Diego: Academic; 2006. p. 596–8.
7. Timmermann L, Gross J, Butz M, Kircheis G, Haussinger D, Schnitzler A. Mini-asterixis in hepatic encephalopathy induced by pathologic thalamo-motor-cortical coupling. Neurology 2003;61:689–92.
8. Lockwood AH, Weissenborn K, Bokemeyer M, Tietge U, Burchert W. Correlations between cerebral glucose metabolism and neuropsychological test performance in nonalcoholic cirrhotics. Metab Brain Dis 2002;17:29–40.
9. Zafiris O, Kircheis G, Rood HA, Boers F, Haussinger D, Zilles K. Neural mechanism underlying impaired visual judgement in the dysmetabolic brain: an fMRI study. Neuroimage 2004;22:541–52.
10. Kircheis G, Wettstein M, Timmermann L, Schnitzler A, Haussinger D. Critical flicker frequency for quantification of low-grade hepatic encephalopathy. Hepatology 2002;35:357–66.
11. O'Carroll RE, Hayes PC, Ebmeier KP, Dougall N, Murray C, Best JJ, et al. Regional cerebral blood flow and cognitive function in patients with chronic liver disease. Lancet 1991;337:1250–3.
12. Shawcross D, Jalan R. Dispelling myths in the treatment of hepatic encephalopathy. Lancet 2005;365:431–33.
13. Riordan SM, Williams R. Treatment of hepatic encephalopathy. N Engl J Med 1997;337:473–9.
14. Song G, Dhodda VK, Blei AT, Dempsey RJ, Rao VL. GeneChip analysis shows altered mRNA expression of transcripts of neurotransmitter and signal transduction pathways in the cerebral cortex of portacaval shunted rats. J Neurosci Res 2002;68:730–7.
15. Brambilla D, Chapman D, Greene R. Adenosine mediation of presynaptic feedback inhibition of glutamate release. Neuron 2005;46:275–83.
16. Jodynis-Liebert J, Flieger J, Matuszewska A, Juszczyk J. Serum metabolite/caffeine ratios as a test for liver function. J Clin Pharmacol 2004;44:338–47.
17. Basheer R, Strecker RE, Thakkar MM, McCarley RW. Adenosine and sleep–wake regulation. Prog Neurobiol 2004;73:379–96.
18. Cordoba J, Cabrera J, Lataif L, Penev P, Zee P, Blei AT. High prevalence of sleep disturbance in cirrhosis. Hepatology 1998;27:339–45.
19. Schneider C, Fulda S, Schulz H. Daytime variation in performance and tiredness/sleepiness ratings in patients with insomnia, narcolepsy, sleep apnea and normal controls. J Sleep Res 2004;13:373–83.
20. Dunwiddie TV, Masino SA. The role and regulation of adenosine in the central nervous system. Annu Rev Neurosci 2001;24:31–55.
21. Santschi LA, Zhang XL, Stanton PK. Activation of receptors negatively coupled to adenylate cyclase is required for induction of long-term synaptic depression at Schaffer collateral-CA1 synapses. J Neurobiol 2006;66:205–19.
22. Rodrigo R, Montoliu C, Chatauret N, Butterworth R, Behrends S, Del Olmo JA, et al. Alterations in soluble guanylate cyclase content and modulation by nitric oxide in liver disease. Neurochem Int 2004;45:947–53.
23. Holschbach MH, Olsson RA, Bier D, Wutz W, Sihver W, Schuller M, et al. Synthesis and evaluation of no-carrier-added 8-cyclopentyl-3-(3-[(18)F]fluoropropyl)-1-propylxanthine ([(18)F]CPFPX): a potent and selective A(1)-adenosine receptor antagonist for in vivo imaging. J Med Chem 2002;45:5150–56.
24. Conn HO. Quantifying the severity of hepatic encephalopathy. In: Conn HO, Bircher J, editors. Hepatic encephalopathy: syndromes and therapies. East Lansing, MI: Medi-Ed; 1993. p. 13–26.
25. Burger C, Buck A. Requirements and implementation of a flexible kinetic modeling tool. J Nucl Med 1997;38:1818–23.
26. Meyer PT, Elmenhorst D, Boy C, Winz O, Matusch A, Zilles K, et al. Effect of aging on cerebral A(1) adenosine receptors: A [(18)F] CPFPX PET study in humans. Neurobiol Aging 2006; DOI 10.1016/j.neurobiolaging.2006.08.005.

27. Svenningsson P, Hall H, Sedvall G, Fredholm BB. Distribution of adenosine receptors in the postmortem human brain: an extended autoradiographic study. Synapse 1997;27:322–35.
28. Logan J, Fowler JS, Volkow ND, Wang GJ, Ding YS, Alexoff DL. Distribution volume ratios without blood sampling from graphical analysis of PET data. J Cereb Blood Flow Metab 1996;16:834–40.
29. Bauer A, Holschbach MH, Meyer PT, Boy C, Herzog H, Olsson RA, et al. In vivo imaging of adenosine A1 receptors in the human brain with [18F]CPFPX and positron emission tomography. Neuroimage 2003;19:1760–9.
30. Meyer PT, Elmenhorst D, Bier D, Holschbach MH, Matusch A, Coenen HH, et al. Quantification of cerebral A1 adenosine receptors in humans using [18F]CPFPX and PET: an equilibrium approach. Neuroimage 2005;24:1192–204.
31. Meyer PT, Bier D, Holschbach MH, Boy C, Olsson RA, Coenen HH, et al. Quantification of cerebral A1 adenosine receptors in humans using [18F]CPFPX and PET. J Cereb Blood Flow Metab 2004;24:323–33.
32. Meyer PT, Elmenhorst D, Matusch A, Winz O, Zilles K, Bauer A. A1 adenosine receptor PET using [18F]CPFPX: displacement studies in humans. Neuroimage 2006;32:1100–5.
33. Meyer PT, Elmenhorst D, Zilles K, Bauer A. Simplified quantification of cerebral A1 adenosine receptors using [18F]CPFPX and PET: analyses based on venous blood sampling. Synapse 2005;55:212–23.
34. Elmenhorst D, Meyer PT, Matusch A, Winz OH, Zilles K, Bauer A. Test–retest stability of cerebral A(1) adenosine receptor quantification using [(18)F]CPFPX and PET. Eur J Nucl Med Mol Imaging 2007;34:1061–70.
35. Matusch A, Meyer PT, Bier D, Holschbach MH, Woitalla D, Elmenhorst D, et al. Metabolism of the A1 adenosine receptor PET ligand [18F]CPFPX by CYP1A2: implications for bolus/infusion PET studies. Nucl Med Biol 2006;33:891–8.
36. Kril JJ, Butterworth RF. Diencephalic and cerebellar pathology in alcoholic and nonalcoholic patients with end-stage liver disease. Hepatology 1997;26:837–41.
37. Meerlo P, Roman V, Farkas E, Keijser JN, Nyakas C, Luiten PG. Ageing-related decline in adenosine A1 receptor binding in the rat brain: an autoradiographic study. J Neurosci Res 2004;78:742–8.
38. Shah NJ, Neeb H, Zaitsev M, Steinhoff S, Kircheis G, Amunts K, et al. Quantitative T1 mapping of hepatic encephalopathy using magnetic resonance imaging. Hepatology 2003 Nov;38:1219–26.
39. Kril JJ, Halliday GM. Brain shrinkage in alcoholics: a decade on and what have we learned? Prog Neurobiol 1999;58:381–7.
40. Gao Z, Robeva AS, Linden J. Purification of A1 adenosine receptor-G-protein complexes: effects of receptor down-regulation and phosphorylation on coupling. Biochem J 1999;338:729–36.
41. Palomero-Gallagher N, Reiffenberger G, Kostopulos G, Kircheis G, Haussinger D, Zilles K. Neurotransmitter receptor alterations in hepatic encephalopathy. In: Haussinger D, Kirchels G, Schliess F, editors. Hepatic encephalopathy and nitrogen metabolism. Dordrecht: Springer; 2006. p. 255–72.
42. Keiding S, Sorensen M, Bender D, Munk OL, Ott P, Vilstrup H. Brain metabolism of 13N-ammonia during acute hepatic encephalopathy in cirrhosis measured by positron emission tomography. Hepatology 2006;43:42–50.
43. Vogels BA, Maas MA, Daalhuisen J, Quack G, Chamuleau RA. Memantine, a noncompetitive NMDA receptor antagonist improves hyperammonemia-induced encephalopathy and acute hepatic encephalopathy in rats. Hepatology 1997;25:820–7.
44. Erceg S, Monfort P, Hernandez-Viadel M, Rodrigo R, Montoliu C, Felipo V. Oral administration of sildenafil restores learning ability in rats with hyperammonemia and with portacaval shunts. Hepatology 2005;41:299–306.